Contract No.:

This manuscript has been authored by Savannah River Nuclear Solutions (SRNS), LLC under Contract No. DE-AC09-08SR22470 with the U.S. Department of Energy (DOE) Office of Environmental Management (EM).

Synthesis and Characterization of Novel Nanothermometers

Delphine Baumert
Savannah River National Laboratory,
Savannah River Site
Aiken, SC 29803

Faculty Advisor: Dr. Simona Hunyadi Murph

Abstract

Nanothermometers enable the measurement of local temperatures at nanoscale dimensions (1-100 nm), which is an important parameter for many biological and industrial applications. One type of nanothermometer is a molecular beacon, which is a stem-loop DNA that contains a fluorophore on one end and a quencher on the other. The temperature response of the nanothermometer is dependent on the melting temperature of the stem-loop which can be altered by modifying the sequence of the DNA strand. Stem loop DNAs can be functionalized onto noble metal nanoparticles to tune the NPs properties and functionalities and obtain real-time, local surface temperature information. This is possible because when the DNA is below its melting point, and the fluorophore is close in proximity to the surface of the NP, the fluorescence is quenched; whereas when the temperature is above the DNAs melting temperature the fluorophore is no longer in the quenching proximity of the NP and a fluorescent signal is observed. Nanoscale noble metals, including Au and Pd are have unique properties that are different than the bulk, which make them more efficient catalysts, more sensitive sensors and more biologically robust materials. Fe_2O_3 nanoparticles have strong magnetic and photocatalytic properties. NPs containing Au, Pd and/or Fe_2O_3 can be heated locally using various techniques, which carries a variety of applications. One drawback of these techniques is the inability to measure the NPs temperature when they are subject to local heating methods. To create multifunctional nanothermometers, we have synthesized a variety of NPs, including Au, Au-Fe_2O_3, Pd, Pd-Fe_2O_3, and Au-Pd-Fe_2O_3 nanoparticles, and attached fluorescently modified stem loop DNA via a thiol attachment. The goal of this work is to measure the local surface temperature of the nanoparticles in a variety of heating techniques. The nanothermometers were characterized using fluorescence spectroscopy, scanning electron microscopy (SEM), UV-Vis spectroscopy, dynamic light scattering (DLS) and phase analysis light scattering (PALS).

Keywords: Nanotechnology, nanothermometers, plasmonic heating

1. Introduction

Nanoparticles have been around since ancient times.[1,2] For example, a cup manufactured by the Romans in the fourth century appears green under normal conditions, but changes to red when illuminated from the inside.[1-3] This phenomenon is a result of the plasmonic properties of the gold and silver nanoparticles (AuNPs) that were used to color the glass.[1-3] In 1847, Michael Faraday made one of the first big steps in nanoparticle (NP) research when he studied the interaction of light and metal NPs and realized that colloidal gold solutions do not exhibit the same properties as bulk gold.[1,4,5] The unique properties that arise due to the large surface area to volume ratios and quantum size effects at the nanoscale expands the use of these materials. For example, inert materials can become efficient catalysts, insulators can grow highly conductive, and opaque substances can appear transparent.[1,6,7]

AuNPs' interesting optical properties arise from the oscillation of electrons on the surface called the localized surface plasmon resonance (LSPR), which make them extremely efficient for sensing, imaging or biological applications.[8] The plasmon band is dependent on the NPs size, shape, and composition.[8] When AuNPs are excited with a laser, visible or near-infrared (NIR) light is converted to heat through non-radiative relaxation of the excited LSPR.[8,9] This method, called plasmonic heating, causes the NPs to

be directly heated rather than through heat transfer from the solvent as in bulk heating, (Figure 1). Currently there are no direct methods of measuring the temperature of plasmonically heated nanomaterials, though temperature predictions have been made through plasmonically heating AuNPs suspended in ice.[10] Due to AuNPs emerging use in photothermal therapy, it is of interest to devise a way to determine the temperature at the surface of a NP. This can lead to applications that involve thermal ablasion of tumor cells for cancer therapy or give real time *in vivo* temperature information.[10-14]

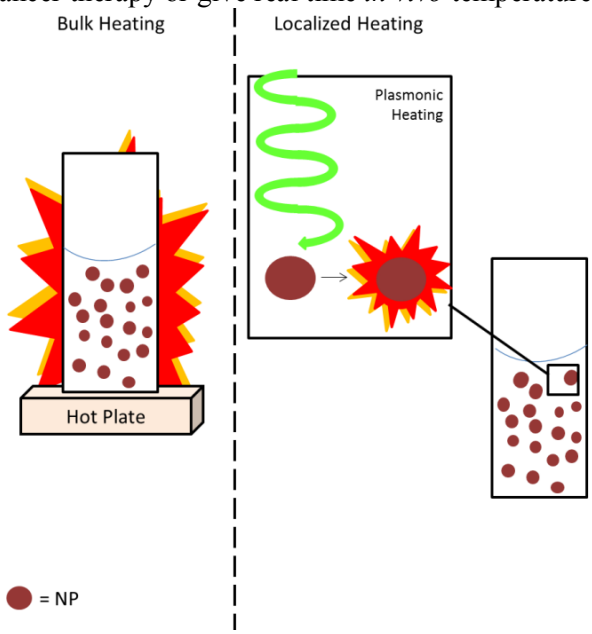

Figure 1. Bulk heating of NPs can be achieved simply through the use of a hot plate, or the direct use of heat to raise the temperature of the NPs through raising the temperature of the entire solution. Localized heating can be achieved through plasmonic heating, where visible or NIR light is converted to heat through nonradiative relaxation of the excited LSPR.

AuNPs have been functionalized with a variety of surface molecules, including DNA, to couple the optical properties of the NPs to the base pairing specific properties of the DNA. Since Mirkin's original experiment in 1995, which conjugated DNA to AuNPs, many variations have been explored, resulting in a wide variety of applications.[14,15] For example, Rinnan et al. reported that DNA functionalized AuNPs can be used as thermometers to measure temperatures in the range of range of 20-60 °C at micro and nanoscales.[14] Although most experiments focus on using AuNPs, Au-Fe_2O_3, Pd, Pd-Fe_2O_3 and Au-Pd-Fe_2O_3 NPs are of emerging interest due to their ability to be locally heated, where the particles themselves are a different temperature than the surrounding bulk material.

Since the heating originates from the NP rather than the solvent, the NP surface is at a higher temperature than the bulk. Due to the small NP size, the surface temperature cannot be measured directly. To overcome this limitation, we took advantage of the highly programmable melting temperature of DNA. In this work, a variety of DNA functionalized nanoparticles, including Au-Fe_2O_3, Pd, Pd-Fe_2O_3 and Au-Pd-Fe_2O_3 NPs were synthesized to create DNA based nanothermometers. The temperature of the nanoparticle surface was measured through the DNA melting temperatures.

The nanothermometers are based on stem loop (SL) DNA molecules that contain a self-complementary 'stem' region and unpaired oligonucleotides in the 'loop' (Figure 2). SL DNA can be unwound to form single stranded DNA at the melting temperature (T_m), which is dependent on the sequence of a particular SL. The T_m can be tuned by changing the length and sequence of the stem and loop, ratio of A-T and G-C bps, introducing mismatch base pairs, and changing salt concentration. In this work, the DNA was modified on one end with a thiol to create reactivity towards the nanoparticle (Figure 2a) and on the other end with a fluorophore, that was used as a fluorescent probe.[14,17,18]. Below the T_m, all

of the DNA molecules are in the closed form. This causes the fluorophore to be quenched through nanometal surface energy transfer (NSET) in the vicinity of the NP surface.[19] As the temperature increases towards the DNA's melting temperature, the DNA begins to unfold in a predictable manner (Figure 2b). Fluorescence increases sharply around the T_m, when the fluorophore moves away from the quenching surface of the NP, exhibiting a sigmoidal rise in intensity as the temperature is increased; this can then be observed using fluorescence spectroscopy (Figure 2c).

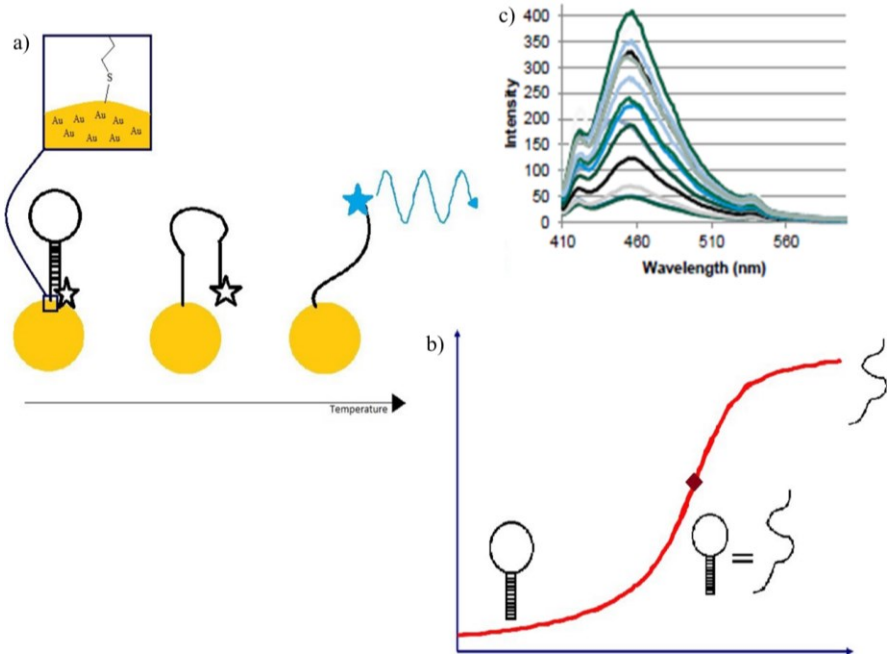

Figure 2. Schematic diagram of the basic idea of the nanothermometer.

2. Materials and Methods

2.1 Materials.

Tris(2-carboxyethyl)phosphine hydrochloride (TCEP), sodium acetate buffer solution, phosphate buffer solution (PBS), sodium dodecyl sulfate (SDS) solution, Tris-EDTA buffer solution, sodium chloride, sodium citrate tribasic dihydrate, gold(III) chloride trihydrate ($HAuCl_4$), iron(III) oxide, and concentrated nitric and hydrochloric acid were purchased from Sigma-Aldrich. All oligonucleotides were purchased from Sigma-Aldrich and were used as received.

2.2 NP synthesis.

Spherical Au NPs were prepared by a citrate reduction approach as reported earlier by our group.[20] Specifically, 0.125 mM $HAuCl_4$ was heated to boiling and 1% (w/v) sodium citrate solution was added. The boiling was continued until the solution turned ruby red, indicating the formation of gold nanoparticles. The resulting nanoparticles were purified by centrifugation and re-dispersion in deionized (DI) water. Pd NPs were produced in the same manner, replacing Au^{3+} with Pd^{2+}.

Au-Fe_2O_3 NPs (or Pd-Fe_2O_3 NPs) were synthesized by first combining 10 µL of a 25 mM Fe_2O_3 NP stock with 10 mL DI water, and heating with stirring for 5 minutes. Then 1 mL of a 1% (w/v) sodium citrate solution was added and the mixture was brought to a boil. Then 250 µL of a 0.01 M $HAuCl_4$ (or 250 µL 0.01 M H_2PdCl_4 in the case of Pd-Fe_2O_3) solution was added and the mixture was heated with stirring at 100°C for 10 minutes. The resulting suspension was then cooled and purified by centrifugation, and re-dispersed in DI water.

Au-Pd-Fe_2O_3 NPs were synthesized by first adding 2 mL of an unwashed Au-Fe_2O_3 suspension and 4.5 mL DI water to a 25 mL Erlenmeyer flask. Then, 0.5 mL of 0.1 M ascorbic acid was added, followed by a stepwise addition of 8.6 μL of 0.01 M H_2PdCl_4 every 5 minutes until 86 μL has been added. The mixture was then stirred for 30 minutes at room temperature to complete the reaction. The particles were then purified by centrifugation.

2.3 Nanothermometer synthesis.

First, the disulfide bond of the thiolated DNAs was reduced overnight at room temperature in the presence of freshly prepared 0.1 M TCEP and 0.5 M sodium acetate buffer (pH 5.2). Next, solutions of freshly activated thiol modified DNA and oligoT helper strand (Table 1) were then added to 1000 μL suspension of NP's in 10 mM phosphate buffered saline (pH 7.7) containing 0.01% (v/v) SDS. The final concentrations of the DNA and helper strand were 2 μM and 1 μM, respectively. To allow self-assembly of the DNAs through the formation of an Au-S or Pd-S bond, the DNA, helper strand and NP were incubated at room temperature for 25 min with gentle shaking. To ensure maximal loading of DNA to the NP, the concentration of sodium chloride was then increased step-wise using a 2.0 M stock solution, in increments of 50 μL until a concentration of 1.0 M was achieved.[21] The mixture was then incubated with gentle shaking for 12 hours at ambient temperature between each addition of salt. Upon completion of the salt aging step, the mixture was incubated overnight at room temperature. For Au or Pd NPs, excess oligos were removed by centrifuging the mixture at 9,000 rpm for 7 minutes at 10°C. For Au-Fe_2O_3, Pd-Fe_2O_3 and Au-Pd-Fe_2O_3 NPs excess oligos were removed through magnetic separation, using a Nd magnet. The mixture was then washed three times with 0.01% SDS, and the NPs were finally dispersed into 1000 μL of measurement buffer (0.3 M NaCl, 10 mM PBS, pH 7.7).

2.4 Fluorescence Measurements.

Fluorescence measurements were performed using a house built instrument. Pacific Blue was excited using a UV lamp (390 nm), and the fluorescence emission spectra were collected from 400-600 nm. The nanothermometers were suspended in measurement buffer (0.3 M NaCl, 10 mM PBS, pH 7.7) and heated using a CUV-QPOD temperature controlled cuvette holder. Measurements were collected with at least 1 mL sample volume in 1.00 cm path length plastic cuvettes from 10-80°C, samples were held at each temperature for at least 10 minutes before each measurement. Melting curves of the NP-DNA conjugates were obtained by plotting the fluorescence intensity at the maximum wavelength against the temperature of the measurement.

2.5 Scanning Electron Microscopy.

Nanothermometers were imaged with scanning electron microscopy and energy dispersive x-ray spectroscopy using a Hitachi SU8230 Scanning Electron Microscope. The nanothermometers were washed with pure water to remove NaCl; then 10 μL was placed on Carbon Type-B 400 Mesh Copper Grids and allowed to dry for several hours at room temperature. Images were acquired at 15 kV and a working distance of 10 mm.

3. Results and Discussion

3.1 Stem Loop DNA Design.

First, the ability of Au-Fe_2O_3, Pd, Pd-Fe_2O_3, and Au-Pd-Fe_2O_3 nanoparticles to be used as nanothermometers was investigated using three SLs and a short DNA fragment that acted as a spacer oligonucleotides were attached to the surface through thiol-metal bonds (Figure 3).[16] In order to increase the temperature range of these nanothermometers, two additional oligonucleotides were designed with different melting temperatures. Our target thermometry range is much higher than that of the previously

reported nanothermometers (>100°C), in order to measure the surface temperature of the AuNP when subjected to plasmonic heating, so we chose target melting points of 80°C and 100°C in the design of the corresponding SLs.

AuNPs are most efficient at quenching the fluorophore at distances of less than 5 nm, so the SLs were designed in a manner such that the fluorophore does not exceed this distance from the NP when the SL is in the closed form (has complementary base pairing, forming a "stem") and the fluorophore sufficiently exceeded this distance from the NP when in the open form (the DNA is now single stranded). [14,16,22] To do this, SLs were designed with longer stems by adding a T_{10} spacer, which has the lowest affinity for the NP surface.[16,23] The increased length and high G-C content, inherently increases the stability and T_m of the SL.

Using these strategies and the help of Integrated DNA Technologies OligoAnalyzer 3.1 online tool, many potential structures were designed, and their optimum secondary structures (Figure 3) and corresponding thermodynamic properties were predicted for the proposed experimental conditions (0.3 M NaCl, 10 mM PBS, pH 7.7). First, a SL with a stem of 25 G-C bps and a loop of 3 nts (ATA) was used (Oligo100). Oligo100 had a predicted T_m of ~100°C under the proposed experimental conditions. Then, while decreasing the stem, the size of the loop was increased to 13 nts, and every other G-C bp in the stem was changed to an A-T bp. This SL had a predicted T_m of ~80°C under proposed experimental conditions. Both of these SLs only had one predicted secondary structure, which is important because the presence of other secondary structures would lead to additional T_m values. The 5' end was functionalized with a variety of fluorophores to simultaneously measure various temperatures on the same NP. The fluorophores used in this study were texas red (TR, λ_{em}=603 nm), Fluorescein (FLC, λ_{em}=522 nm), 5-Fluorescein (FAM, λ_{em}=515 nm) and pacific blue (PB, λ_{em}=451 nm). The 3' end was functionalized with a dithiol to create reactivity toward the NP surface.

Table 1: SL sequences used (5'-3')
OligoT Helper: TTTTTTTTTT-$(CH_2)_3$-SH
OligoF**:** FAM-ATCATAATTATTGTTTTTTTTTTTTTTTACTATTTTTTTGAT-(10T)-$(CH_2)_3$-SH
OligoTR**:** TR-ATCTAATCATTATTGTTTTTTTTTTTTTTTACTATTATGTTTAGAT-(10T)-$(CH_2)_3$-SH
OligoPB**:** PB 425-ATATACATTTGTTTTTTTTTTTTACATATGTATAT-(10T)-$(CH_2)_3$-SH
Oligo80: TR-TGCGCGCGCCGCCGGCGGCCGCCGGCGATACGCCGGCGGCCGCCGGCGGCGCGCGC-(10T)-$(CH_2)_3$-SH
Oligo100: FLC-TGCACTCGCTGTCGGAGGCTGCTATATATAATATAGCAGCCTCCGACAGCGAGTGC-(10T)-$(CH_2)_3$-SH

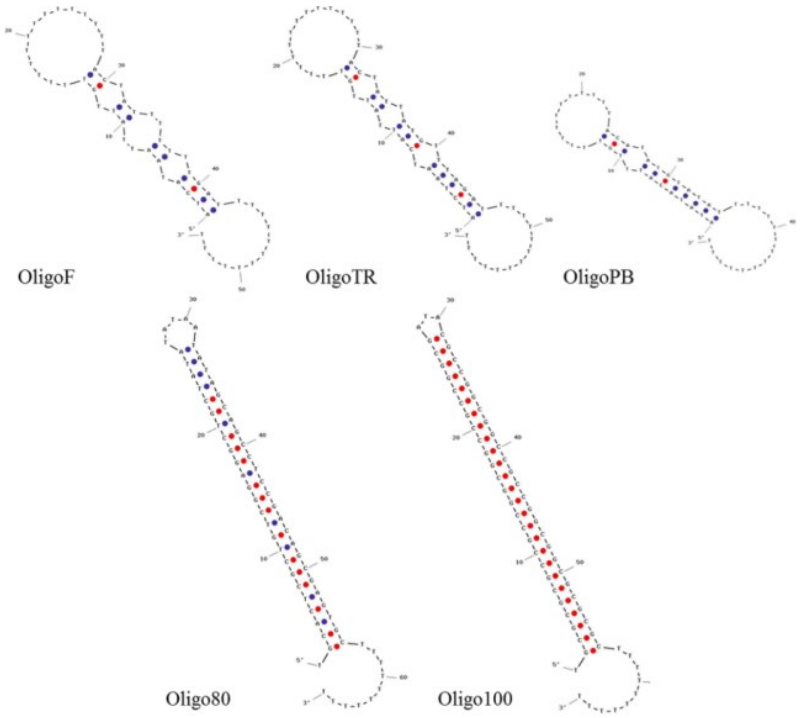

Figure 3. Secondary structures of oligonucleotides used in this study under optimal experimental conditions (0.3 M NaCl, pH 7.7) generated using IDTs OligoAnalyzer.

3.2 Synthesis of nanothermometers.

To synthesis noble metal-DNA conjugates, the disulfide on the 3' end was reduced using tris(2-carboxyethyl)phosphine, a powerful, irreversible reducing agent that does not interact with metals. Next the freshly reduced DNA was incubated with the noble metal NPs, and the sodium concentration was slowly increased up to 1.0 M over the course of 4 days. This salt reduced the for the charge repulsion between the negatively charged DNA backbone to create a higher loading of DNA on the Au and Pd surfaces.

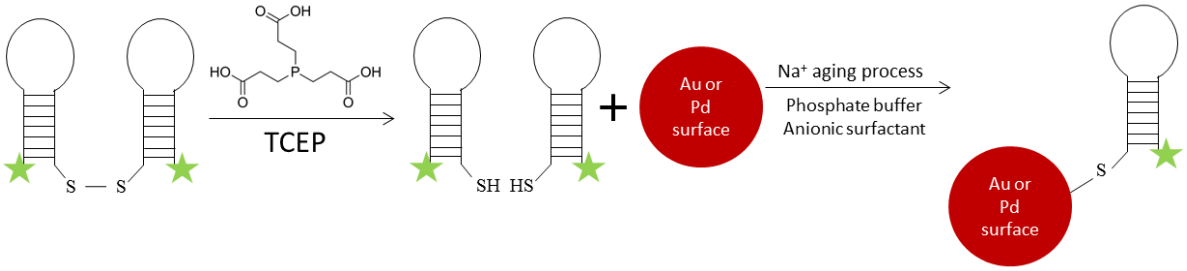

Figure 4. Reaction scheme for the functionalization of noble metal NPs with fluorescent stem loop DNA.

3.3 Characterization of NPs and NP-DNA conjugates.

The size and shape of the synthesized Au, Au-Fe_2O_3, Pd, Pd-Fe_2O_3, and Au-Pd-Fe_2O_3 NPs before and after their DNA functionalization were evaluated using scanning electron microscopy (SEM). Energy dispersive X-ray spectroscopy (EDS), a technique that measures characteristic X-rays to provide localized elemental information, was used concurrently with the SEM to give characteristic elemental data at localized points on the micrograph.[24]

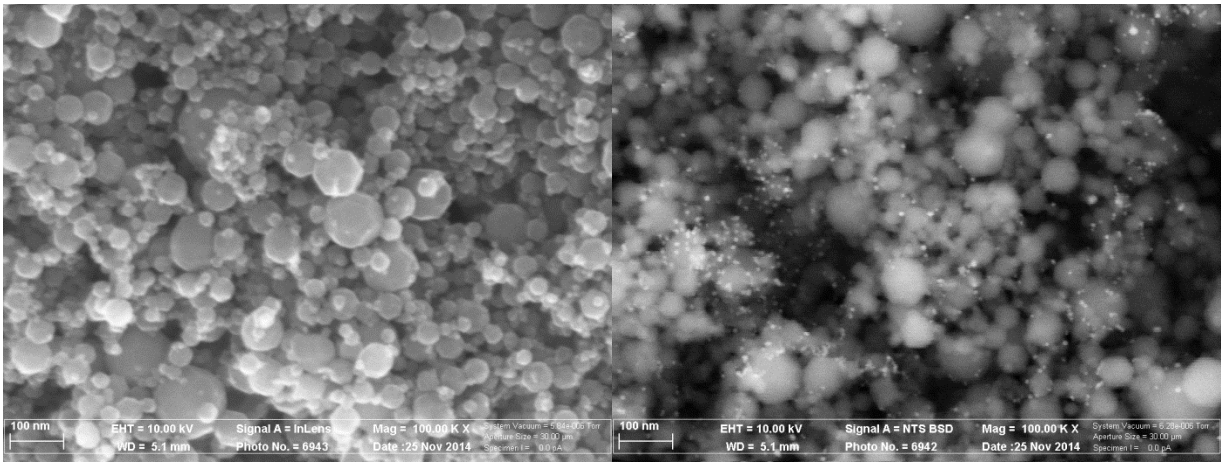

Figure 5. SEM micrograph of Au-Fe_2O_3 NPs. Fe_2O_3 NPs are approximately 50 nm, and AuNPs are approximately 20 nm.

The NPs and NP-DNA conjugates optical properties were evaluated via UV-Vis spectroscopy. Size and shape of NPs affects their optical properties, specifically localized surface plasmon resonance (LSPR) wavelengths, which can be observed as large absorption peaks in either the visible or NIR region of the spectrum.[1,4] For AuNPs, these properties have been widely characterized and visible spectroscopy is used to determine the size and concentration of AuNPs.[25] AuNPs exhibit LSPR, which is dependent on the size and shape of the NPs. In AuNPs, the LSPR wavelength can be tuned by varying the size between 1-100 nm.[25] The AuNPs used were approximately 20 nm, and therefore had plasmon peaks around 520 nm. Pd lacks any characteristic peaks in the UV-Vis spectrum, though it has been reported to also potentially exhibit plasmonic properties.[26] Fe_2O_3 NPs absorb strongly in the UV region, which was used to confirm its presence (Figure 6). Additionally, the success of DNA conjugation to a NP was monitored with UV spectroscopy, making use of DNA's absorbance at 260 nm.

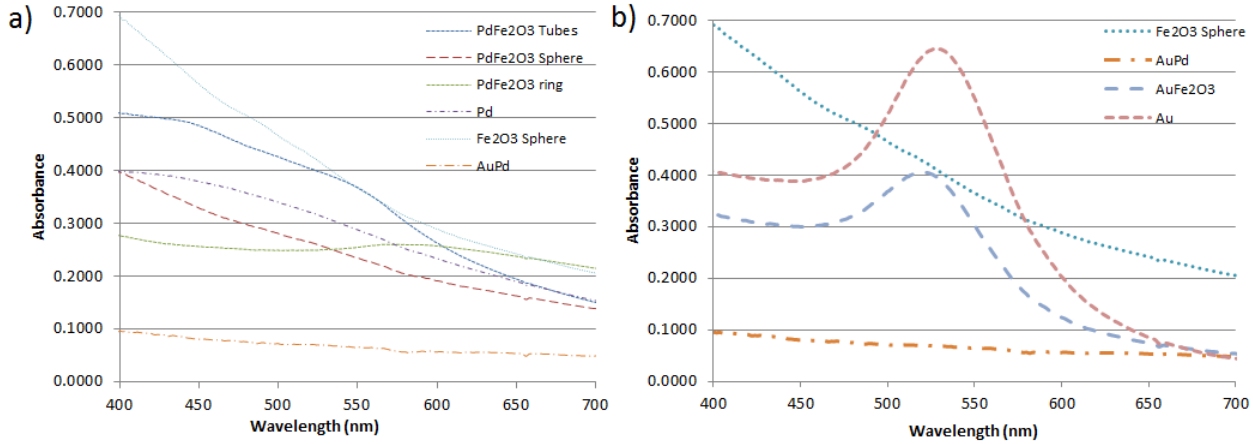

Figure 6. a) UV-Vis spectra of all Pd NPs. b) UV-Vis spectra of all Au NPs. All measurement were acquired in quartz cuvettes, pathlength 1.00 cm

The NP-DNA conjugate's ability to function as a nanothermometer was assessed using fluorescence spectroscopy. Each NP-DNA conjugate was excited at the fluorophore's specific excitation wavelength and the emission spectra of the fluorophores were recorded while bulk heating was applied to the solution. The maximum emission wavelength was plotted against temperature and resulted in the expected sigmoidal melting curve for each nanothermometer (Figure 7).

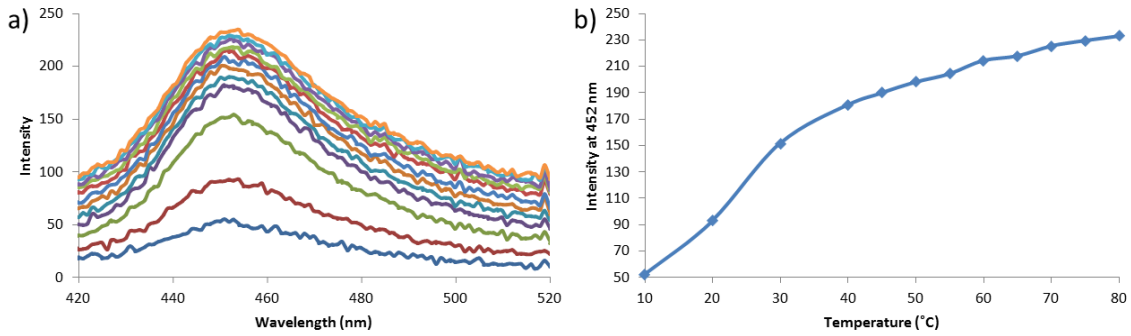

Figure 7. a) Fluorescence emission spectra of Au-OligoPB (0.3 M NaCl, pH 7.4) as temperature rises. An excitation energy of 395 nm was used. b) Intensity of fluoresence of Au-OligoPB at 452 nm as a function of temperature.

4. Conclusion

A straightforward approach was developed for the synthesis of Pd, Pd-Fe_2O_3, Au-Fe_2O_3, and Au-Pd-Fe_2O_3 nanothermometers, using a single SL DNA. These NP-DNA conjugates were characterized using techniques including EDX measurements, scanning electron microscopy and fluorescence spectroscopy. The fluorescence studies of the NP-DNA demonstrated that all of the tested nanomaterials can serve as anchors of DNA, and thus this system can be used to measure local temperatures.

5. Future Work

Currently we are working on setting up a new custom portable fluorescence measurement system, which will allow us to evaluate other fluorophores that are excited at wavelengths higher than 400 nm in the presence of the heating technique. We are continuing on the optimization of the synthesis of nanothermometers using Pd, Pd-Fe_2O_3, Au-Fe_2O_3, and Au-Pd-Fe_2O_3 NPs. While this report focuses primarily on the ability of one type of DNA strand to be functionalized to a NP and be used as a nanothermometer, the overall goal is to create a multiplex nanostructure, where a NP with many different DNAs attached is used to assess a wide range of temperatures on the same NP surface.[16] Additionally, we hope to soon begin using these nanothermometers to give us local temperature information of our NPs in local heating experiments in our lab.

6. Acknowledgements

Thank you Dr. Newton and Augusta University for supporting an internship experience at Savannah River National Lab (SRNL). Thank you DOE-SRNL LDRD for providing the financial, materials, and technical support of this research work. Thank you to Sarah Schyck for synthesizing the NPs used in these experiments, and to Dr. Larsen and Dr. Coopersmith for all of the help in the lab.

7. References

1. Heiligtag, F. J.; Niederberger, M. The Fascinating World of Nanoparticle Research. *Materials Today*. **2013**, *16*, 262–271.
2. Barber, D. J.; Freestone, I. C. *Archaeometry* **1990**, *32* (1), 33–45.
3. Freestone, I.; Meeks, N.; Sax, M.; Higgitt, C. The Lycurgus Cup — A Roman Nanotechnology. *Gold Bulletin Gold Bull*. **2007**, *40*, 270–277.
4. Giljohann, D. A.; Dwight S. Seferos, D. S.; Daniel, W. L.; Massich, M. D.; Patel, P. C.; Mirkin, C. A. Gold Nanoparticles For Biology and Medicine. *Angewandte Chemie International Edition*. **2010**, 3280–3294.
5. Mody, V.; Siwale, R.; Singh, A.; Mody, H. Introduction To Metallic Nanoparticles. *Journal of Pharmacy and Bioallied Sciences J Pharm Bioall Sci*. **2010**, *2*, 282.

6. Alivisatos, A. P. *Science* **1996**, *271* (5251), 933–937.
7. Polshettiwar, V.; Varma, R. S. *Green Chemistry Green Chem.* **2010**, *12* (5), 743.
8. Aioub, M.; El-Sayed, M. A. A Real-Time Surface Enhanced Raman Spectroscopy Study Of Plasmonic Photothermal Cell Death Using Targeted Gold Nanoparticles. *J. Am. Chem. Soc. Journal of the American Chemical Society*. **2016**, *138*, 1258–1264.
9. Brongersma, M. L.; Halas, N. J.; Nordlander, P. Plasmon-Induced Hot Carrier Science and Technology. *Nature Nanotech Nature Nanotechnology*. **2015**, *10*, 25–34.
10. Govorov, A. O.; Richardson, H. H. Generating Heat with Metal Nanoparticles. *Nano Today*. **2007**, *2*, 30–38. Harada, Y.; Takeuchi, T.; Kino, H.; Fukushima, A.; Takakura, K.; Hieda, K.; Nakao, A.; Shin, S.; Fukuyama, H. Electronic Structure Of DNA Nucleobases and Their Dinucleotides Explored by Soft X-Ray Spectroscopy. *J. Phys. Chem. A The Journal of Physical Chemistry A*. **2006**, *110*, 13227–13231.
11. Xuan, M.; Shao, J.; Dai, L.; Li, J.; He, Q. *ACS Appl. Mater. Interfaces ACS Applied Materials & Interfaces* **2016**, *8* (15), 9610–9618.
12. Azhdarzadeh, M.; Atyabi, F.; Saei, A. A.; Varnamkhasti, B. S.; Omidi, Y.; Fateh, M.; Ghavami, M.; Shanehsazzadeh, S.; Dinarvand, R. *Colloids and Surfaces B: Biointerfaces* **2016**, *143*, 224–232.
13. Hu, Y.; Zhou, Y.; Zhao, N.; Liu, F.; Xu, F.-J. *Small* **2016**, *12* (18), 2459–2468.
14. Liu, H.; Fan, Y.; Wang, J.; Song, Z.; Shi, H.; Han, R.; Sha, Y.; Jiang, Y. *Sci. Rep. Scientific Reports* **2015**, *5*, 14879.
15. Chen, R.; Huang, X.; Xu, H.; Xiong, Y.; Li, Y. Plasmonic Enzyme-Linked Immunosorbent Assay Using Nanospherical Brushes As a Catalase Container for Colorimetric Detection of Ultralow Concentrations of Listeria Monocytogenes. *ACS Appl. Mater. Interfaces ACS Applied Materials & Interfaces*. **2015**, *7*, 28632–28639.
16. Ebrahimi, S.; Akhlaghi, Y.; Kompany-Zareh, M.; Rinnan, Å. Nucleic Acid Based Fluorescent Nanothermometers. *ACS Nano*. **2014**, *8*, 10372–10382.
17. Elghanian, R. Selective Colorimetric Detection of Polynucleotides Based on the Distance-Dependent Optical Properties of Gold Nanoparticles. *Science*. **1997**, *277*, 1078–1081.
18. Love, J. C.; Wolfe, D. B.; Haasch, R.; Chabinyc, M. L.; Paul, K. E.; Whitesides, G. M.; Nuzzo, R. G. Formation And Structure of Self-Assembled Monolayers of Alkanethiolates on Palladium. *J. Am. Chem. Soc. Journal of the American Chemical Society*. **2003**, *125*, 2597–2609.
19. Yun, C. S.; Javier, A.; Jennings, T.; Fisher, M.; Hira, S.; Peterson, S.; Hopkins, B.; Reich, N. O.; Strouse, G. F. Nanometal Surface Energy Transfer In Optical Rulers, Breaking the FRET Barrier. *J. Am. Chem. Soc. Journal of the American Chemical Society*. **2005**, *127*, 3115–3119.
20. Murph, S. E. H.; Larsen, G. K.; Lascola, R. J. *Journal of Visualized Experiments JoVE* **2016**, No. 108.
21. Hurst, S. J.; Lytton-Jean, A. K. R.; Mirkin, C. A. Maximizing DNA Loading On a Range of Gold Nanoparticle Sizes. *Analytical Chemistry Anal. Chem.* **2006**, *78*, 8313–8318.
22. Algar, W. R.; Massey, M.; Krull, U. J. The Application of Quantum Dots, Gold Nanoparticles and Molecular Switches to Optical Nucleic-Acid Diagnostics. *TrAC Trends in Analytical Chemistry*. **2009**, *28*, 292–306.
23. Demers, L. M.; Mirkin, C. A.; Mucic, R. C.; Reynolds, R. A.; Letsinger, R. L.; Elghanian, R.; Viswanadham, G. A Fluorescence-Based Method For Determining the Surface Coverage and Hybridization Efficiency of Thiol-Capped Oligonucleotides Bound to Gold Thin Films and Nanoparticles. *Analytical Chemistry Anal. Chem.* **2000**, *72*, 5535–5541.
24. Hafner, B. Energy Dispersive Spectroscopy On the SEM: A Primer. Characterization Facility, University of Minnesota: Twin Cities.
25. Haiss, W.; Thanh, N. T. K.; Aveyard, J.; Fernig, D. G. Determination Of Size and Concentration of Gold Nanoparticles from UV−Vis Spectra. *Analytical Chemistry Anal. Chem.* **2007**, *79*, 4215–4221.
26. Lu, X.; Rycenga, M.; Skrabalak, S. E.; Wiley, B.; Xia, Y. Chemical Synthesis Of Novel Plasmonic Nanoparticles. *Annual Review of Physical Chemistry Annu. Rev. Phys. Chem.* **2009**, *60*, 167–192.